0012-9402/06/020211-12
DOI 10.1007/s00015-006-1183-z
Birkhäuser Verlag, Basel, 2006

Eclogae geol. Helv. 99 (2006) 211–222

3D modeling and kinematics of the external zone of the French Western Alps (Belledonne and Grand Châtelard Massifs, Maurienne Valley, Savoie)

DIDIER MARQUER[1], PHILIPPE CALCAGNO[2], JEAN-CLAUDE BARFETY[2] & THIERRY BAUDIN[2]

Key words: 3D geometric modeling, shear zones, Miocene tectonics, Western Alps, Belledonne, Grand Châtelard

ABSTRACT

Three dimensional geometric modeling was undertaken on the external crystalline massifs (Belledonne and Grand Châtelard) of the Western Alps. This external zone corresponds to the internal part of the European passive margin developed during Liassic rifting. It was thrust towards the north-west during Oligocene-Miocene compression resulting in tectonic inversion of the European continental margin.

The contact between basement and cover rocks was modeled in three dimensions using 30 cross-sections oriented NW-SE and NE-SW, together with geological outcrops located onto the Digital Elevation Model of the area. Three interfaces in the model correspond to the main geological features: (i) the unconformity between the Triassic series and the metamorphic Palaeozoic basement (generally assumed to have been horizontal at the beginning of the Alpine cycle), (ii) ENE-WSW extensional faults associated with the main stage of passive margin development, and (iii) steep NNE-SSW trending faults that developed during the main compressive stage of Alpine collision.

The Miocene deformation is very heterogeneous and results in networks of anastomosing brittle-ductile shear zones. This deformation corresponds to a NW-SE compression associated with an important vertical stretching in the basement massifs. The eastern border of the Belledonne massif is locally backthrust towards the south-east and shows a bulk dextral shear component.

3D geometric modeling revealed the overall anastomosing shape of the main fault zones, which undulate around vertically stretched crustal-scale basement boudins. Former structures, such as Liassic extensional faults, are preserved within low-strain domains located in the core of these boudins. At lower scale, the 3D model pointed out characteristic locations where the investigated shear zone patterns reveal the bulk Miocene deformation.

RESUME

Une modélisation géométrique tridimensionnelle est réalisée sur une partie des massifs cristallins externes des Alpes occidentales (Belledonne et Grand Châtelard). Cette zone externe correspond à la partie interne de la marge passive européenne formée pendant l'extension liasique. Les massifs cristallins externes sont chevauchants vers le nord-ouest pendant la compression oligo-miocène. Ce chevauchement est responsable de l'inversion de la marge européenne.

La géométrie du contact socle-couverture est modélisée en 3 dimensions à partir de 30 coupes orientées NO-SE et NE-SO et d'affleurements géoréférencés sur le Modèle Numérique de Terrain de la région étudiée. Trois interfaces sont particulièrement représentées dans le modèle 3D: (i) la discordance entre les dépôts du Trias et le socle paléozoïque (considérée comme horizontale au moment des dépôts), (ii) les failles normales, d'orientation ENE-OSO, associées au développement de la marge passive et (iii) les zones de cisaillement et les failles, d'orientation NNE-SSO, développées pendant la période de raccourcissement associée à la collision alpine.

La déformation miocène est hétérogène et conduit à un réseau de zones de cisaillement fragile-ductile anastomosées. Cette déformation correspond à un raccourcissement orienté NO-SE et est associée à un important étirement vertical des massifs. La bordure orientale du massif de Belledonne est localement rétro-chevauchée vers le sud-est et souligne l'influence d'une composante de cisaillement dextre.

La modélisation géométrique 3D révèle la forme globale anastomosée des zones de cisaillement principales qui entourent des lentilles de socle à l'échelle crustale. Certaines structures sont préservées dans les zones de faible déformation au coeur de ces lentilles: par exemple, les failles d'extension liasiques au SO du massif du Grand Châtelard. La modélisation 3D a permis de caractériser des zones-cibles pour l'étude de la géométrie et de la distribution des zones de cisaillement et de définir la cinématique miocène dans cette partie des massifs cristallins externes.

Introduction

The recent development of three dimensional (3D) numerical models for geological interfaces has numerous applications in the earth sciences (Hamilton & Jones 1992; Houlding 1995; Jessell & Valenta 1996; Courrioux et al. 2001). In addition to providing useful geo-referenced data bases, this approach can be used as a tool for three dimensional visualization that can improve large scale geometrical, cartographic and structural models. The compatibility of complex struc-

[1] Université de Franche Comté, Géosciences, 16 route de Gray, F-25030 Besançon, France. E-mail: didier.marquer@univ-fcomte.fr
[2] BRGM Orléans, France. E-mail: p.calcagno@brgm.fr, jc.barfety@brgm.fr and t.baudin@brgm.fr

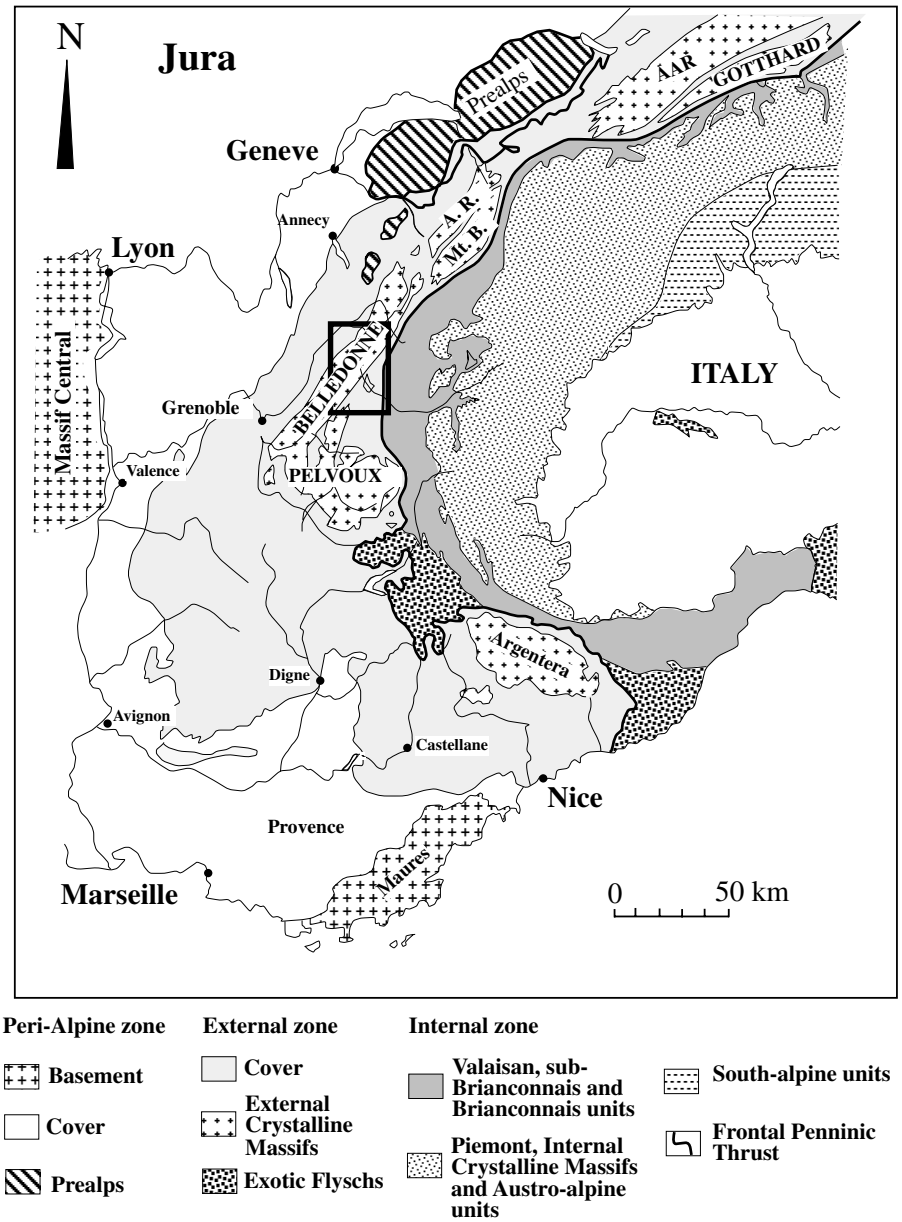

Fig. 1. Location of the study area in the Western Alps (after Debelmas & Kerckhove 1980).

tures and their lateral variations in three dimensions, as well as their volumetric representation and the large-scale geometry of these structures, can be assessed by the use of 3D numerical modeling.

For good constraint, 3D numerical models require areas with high topographic relief. For this reason, a 3D geometrical model was constructed for a wide area of the External Crystalline Massifs (ECM) of the French Western Alps (Fig. 1) (Schmid et al. 2004). The study area included the Belledonne (BM) and Grand Châtelard (GCM) massifs located around the Maurienne valley (Fig. 2), which belong to the internal part of the European passive margin initiated during Liassic rifting of the Tethys and Valaisan oceans (Debelmas & Lemoine 1970; Tricart 2004). This part of the European margin was inverted and thrust north-westwards during the Miocene Alpine compression (Menard & Thouvenot 1987; Menard & Rochette 1992; Crouzet, 1997; Fügenschuh et al. 1999; Ceriani et al. 2001; Bucher et al. 2004; Ceriani & Schmid, 2004).

The paper deals with techniques used for 3D modeling, and the geometry of the main interfaces located both at the boundaries and within the BM and GCM. The problems encountered in constructing the 3D geometrical models and interpreting the geological results are also presented and discussed. These 3D models are tools suited for solving geometrical problems and are important for understanding the geological relationships of complex three dimensional structures. Combined with this 3D modeling, a geometrical and kinematic study of Miocene shear zone patterns is performed to link, at the small scale, the geo-

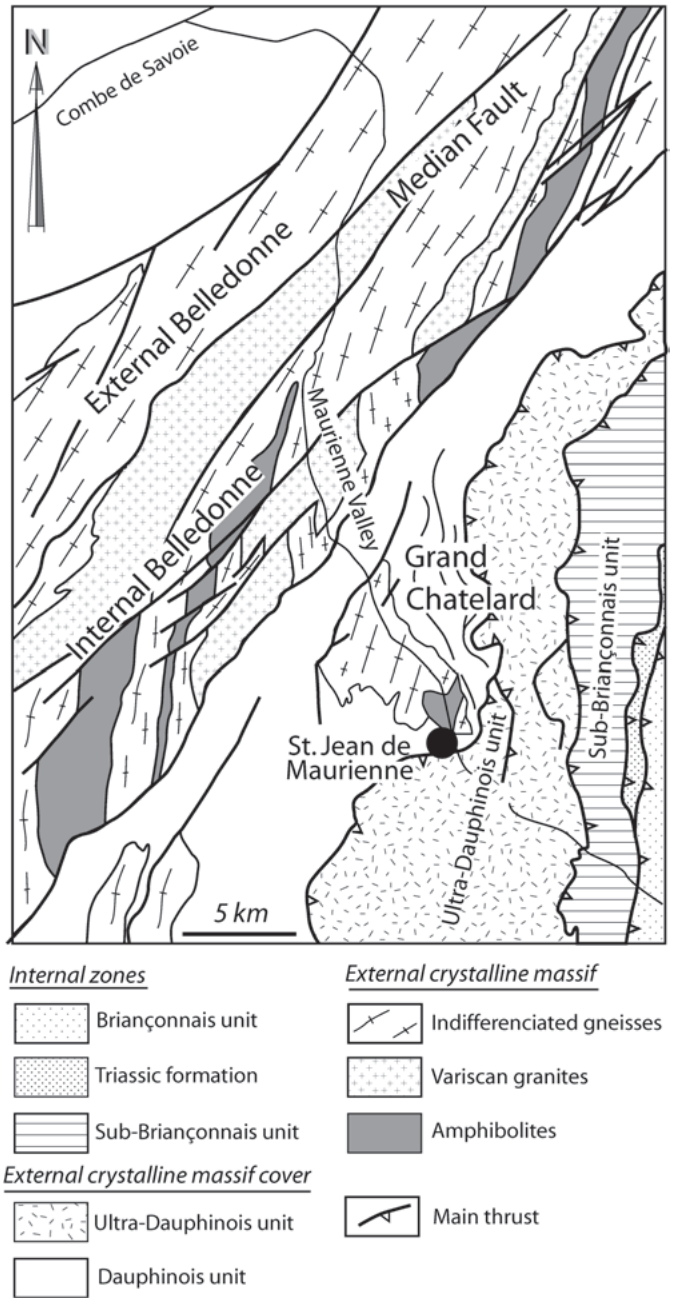

Fig. 2. Simplified geological map and representation of the main interfaces in the Belledonne and Grand Châtelard massifs area.

metry of observed lense-shaped domains of weakly deformed basement with the geometry of Miocene curviplanar thrust interfaces, previously visualised in the 3D model, in the internal parts and at the boundaries of the BM and GCM. The current geometric and kinematic study of the main Miocene interfaces in the basement of the BM and GCM illustrates clearly how this kind of model can be useful for focusing on well-chosen geological targets.

Geological and tectonic setting

The downstream part of the Maurienne valley (or Arc valley) between the Combe de Savoie to the west and the town of Saint-Jean-de-Maurienne to the east (Fig. 2) was selected as a subject for 3D modeling because of its extensive natural sections (altitude difference of 2000 m) and because of its relative structural simplicity compared to the more internal Alpine zones. The area is covered by the 1:50,000-scale geological maps of La Rochette (Barféty et al. 1983) and Saint-Jean-de-Maurienne (Barféty et al. 1977). The Maurienne valley from north to south intersects successively:

- the external cover of the Belledonne massif,
- the Hercynian basement of the Belledonne massif,
- the poorly developed internal cover (Triassic and Lias), and
- a detached cover (Triassic to Tertiary) resting on a second exposure of Hercynian basement: the Grand-Châtelard Massif.

This group of rocks, defined as the Dauphinoise Zone, is overthrust from the east by rocks of the Ultra-Dauphinoise Zone (Carboniferous to Eocene) which forms the limit of the modeled area (Fig. 2).

The Belledonne massif comprises two units, an external branch ("rameau externe") to the west and an internal branch ("rameau interne") to the east, separated by a continuous layer of sedimentary rock (Trias and Lias) known as the median fault ("accident médian").

The eastern sedimentary cover of the Belledone crystalline basement becomes increasingly detached and overlapping (towards the north-west) as one proceeds to the south-east. The Ultra-Dauphinoise Zone, cutting the Arc valley near Saint-Jean-de-Maurienne, is the easternmost part. It is characterized at the top by a transgressive nummulitic flysch (flysch des Aiguilles d'Arves, Priabonien) which overlies previous thrusting and folding structures oriented transverse to the mountain belt (E-W) that probably represent upper Cretaceous deformation (phase "Arvinche"; Barbier 1956).

The tectonic history of the external zone can be summarized as follows:

After the Hercynian belt was leveled during the Permian, the Dauphinois basement was dissected by normal faulting during the Triassic, more particularly during the Jurassic (Barféty 1985), into a succession of blocks prefiguring the present-day external crystalline massifs ("MCE"). These passive margin structures, forming half-grabens, were formed concurrently with a South-Eastern Basin that developed during the Late Jurassic into the Ligurian-Piedmontese domain. The activity of these normal faults, which developed in particular during the Middle Lias, gave rise to the deposition of synsedimentary breccias (Barféty & Gidon 1984) and clastic dykes. These deposits mark one of the normal faults that truncates the southern slopes of the Grand

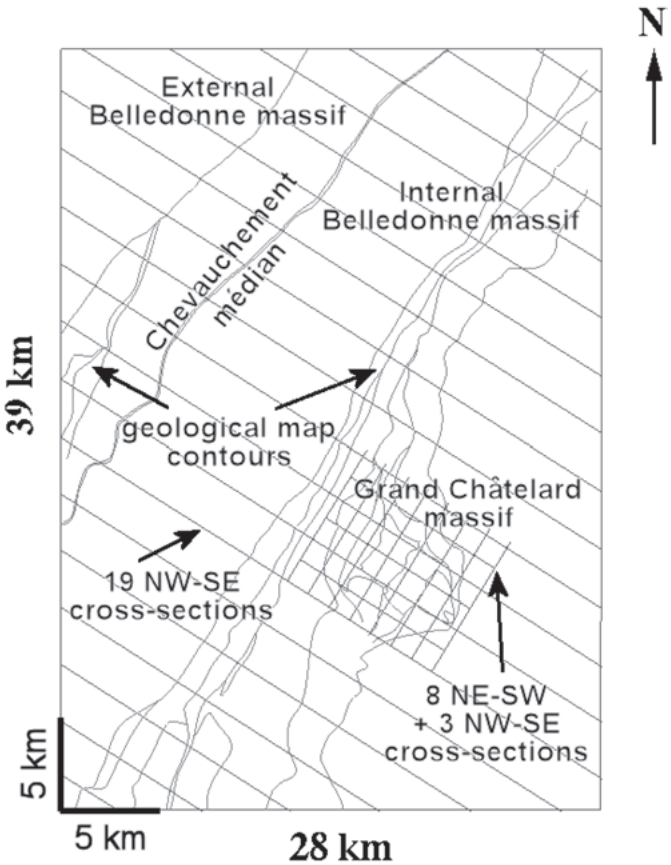

Fig. 3. Location of the cross-sections and geological projection of the Miocene interfaces and the Liassic faults.

Châtelard massif (Barbier 1944; Barféty et al. 1977; Barféty 1985).

Although signs of the early Alpine compressions are apparent farther south in the Taillefer massif (Barféty & Gidon 1990), no clear imprint of this pre-Eocene Arvinche phase is seen in the study area.

Most of the thrust faults affecting the area can be attributed to inversion of the Liassic normal faults during the Oligo-Miocene. Peak Alpine metamorphism recorded in the Belledonne massif (Nziengui 1993) is estimated at T = 320°C to 350°C and P = 230 MPa, with an age around 26 Ma. This metamorphism is directly related to crustal overthickening generated by overthrusting towards the NW (Tricart 2004).

Thermopaleomagnetic records associated with fission-track analyses on apatite indicate that cooling was at first (24 Ma to 21.5 Ma) very rapid and then (20 Ma to 10 Ma) much slower (Crouzet 1997). This result is coherent with published zircon and apatite fission-track data in this Western part of the Alps (Seward & Mancktelow 1994; Fügenschuh et al. 1999; Fügenschuh & Schmid 2003) and part of proposed structural evolution of the neighbouring Mont Blanc Massif (Leloup et al. 2005).

3D models

The 3D geometrical models were constructed with Strim, a computer aided design software, (Strim version 6.1, Matra Division) using a data base of 30 geological cross-sections and geological surfaces located on a digital elevation model (DEM) of the studied area (Lambert 2 projection: Cuenin 1972). The data were entered as curves or surface equations or as points referred to by spatial coordinates. Calculations were done by data interpolations based on Bezier curves or surfaces (Forrest 1990; de Kemp 1999).

Data base

The structural map (Fig. 2) was drawn using 1:50,000-scale geological maps (St. Jean de Maurienne 774, 1977; La Rochette 750, 1983) and field data acquired during the study. The three main geological interfaces were selected in order to ensure good readability from the 3D models. They correspond to distinct geological events: (i) the unconformity between basement rocks and the overlying Triassic cover, which is assumed to have been horizontal at the time of deposition, (ii) Carixian (Early Lias) normal faults which bound the south-west border of the GCM and (iii) the main Miocene thrusts.

This data set, corresponding to the structural map, was drawn using topographic levels from the DEM (Institut Géographique National, France) (Fig. 3). The internal resolution of the DEM is 50 meters and the 3D model is strongly influenced by the smooth relief that results from such broad resolution in some parts of the mapped area. Each point is geo-referenced with X, Y and Z coordinates in the model.

Cross-sections were drawn using geological maps, field data and topographic profiles derived from the DEM, and included geological interface locations. Across the whole area, 19 NW-SE serial cross-sections oriented perpendicular to the main structures were constructed as shown in Figure 3. For the GCM, 3 NW-SE oriented cross-sections and 8 NE-SW oriented cross sections were added in order to better constrain the complex geometry (Fig.3). All the cross-sections were constructed using structural surface data and cartographic contact shapes to define the dip of the interfaces. In some places, an existing Electricité de France gallery allowed corroboration of the dip values.

Method

The structural map and the cross-sections were digitized and recorded in the modeling program as reference points. The DEM was introduced as a grid and the geological interfaces were compiled as Bezier curves. Geometrical effects with wavelengths less than 200 meters are not shown by the model, reflecting the resolution of the DEM grid and the cross-section constructions. The 3D model was constructed

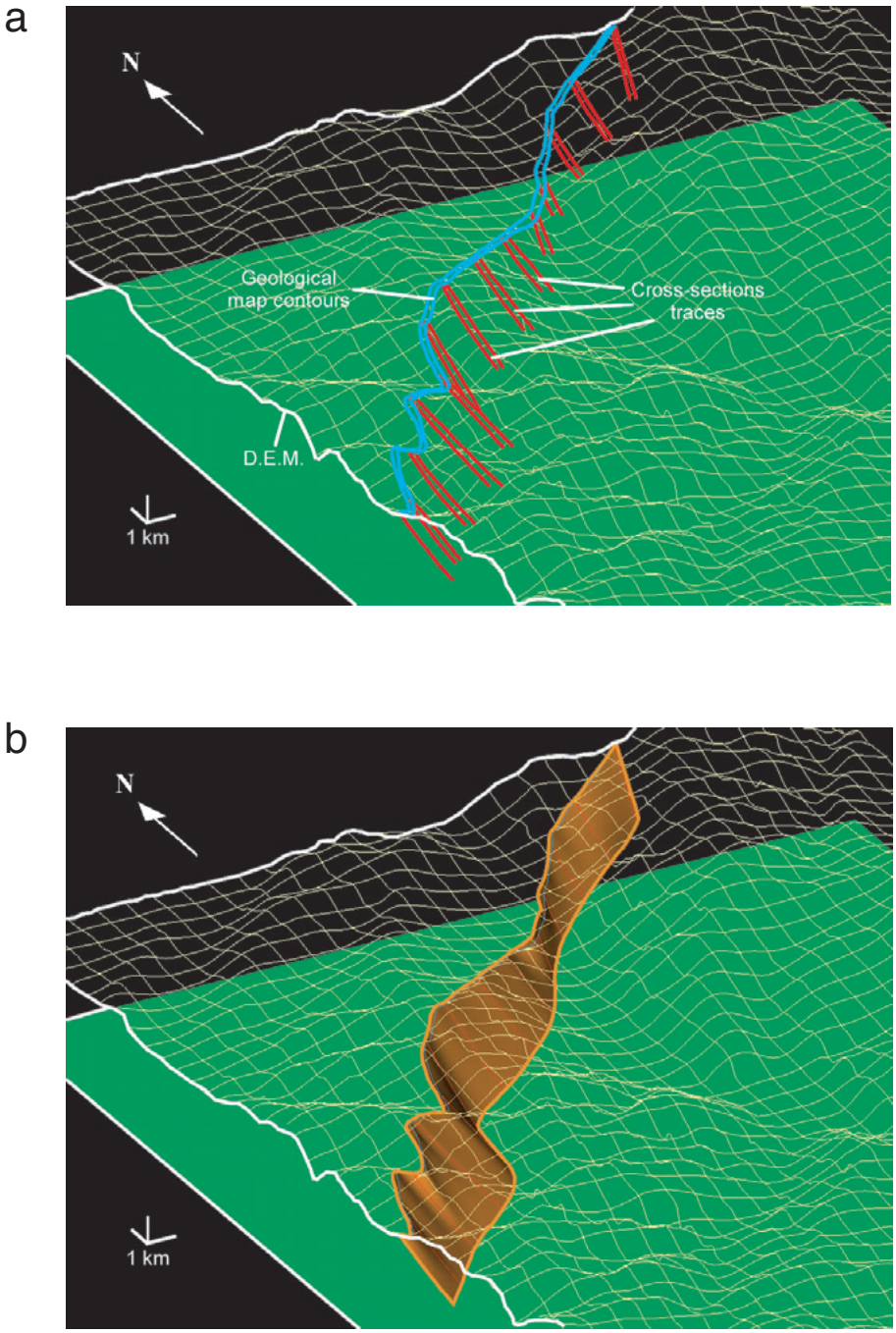

Fig. 4. 3D model of the "accident médian": a) representation of the data used and b) numerical interpolation of the 3D surface.

interactively, because the order in which the different interfaces are built depends on their individual geological history. In other words, the older structures are affected by the more recent ones, and the geometry of the different interfaces depends on the relative timing of their development. For this reason, younger structures were constructed first and were used as boundary conditions for the building of older interfaces.

Numerical modeling of the structural map and cross-sections

The structural map data were put into the 3D software as reference points extracted from the geological contours. The first step was to construct numerical contours from the reference points. This was done initially in an horizontal plane (Z=0) using point interpolation with a Bezier curve function. Then, to get a 3D surface view, the interpolated curves were project-

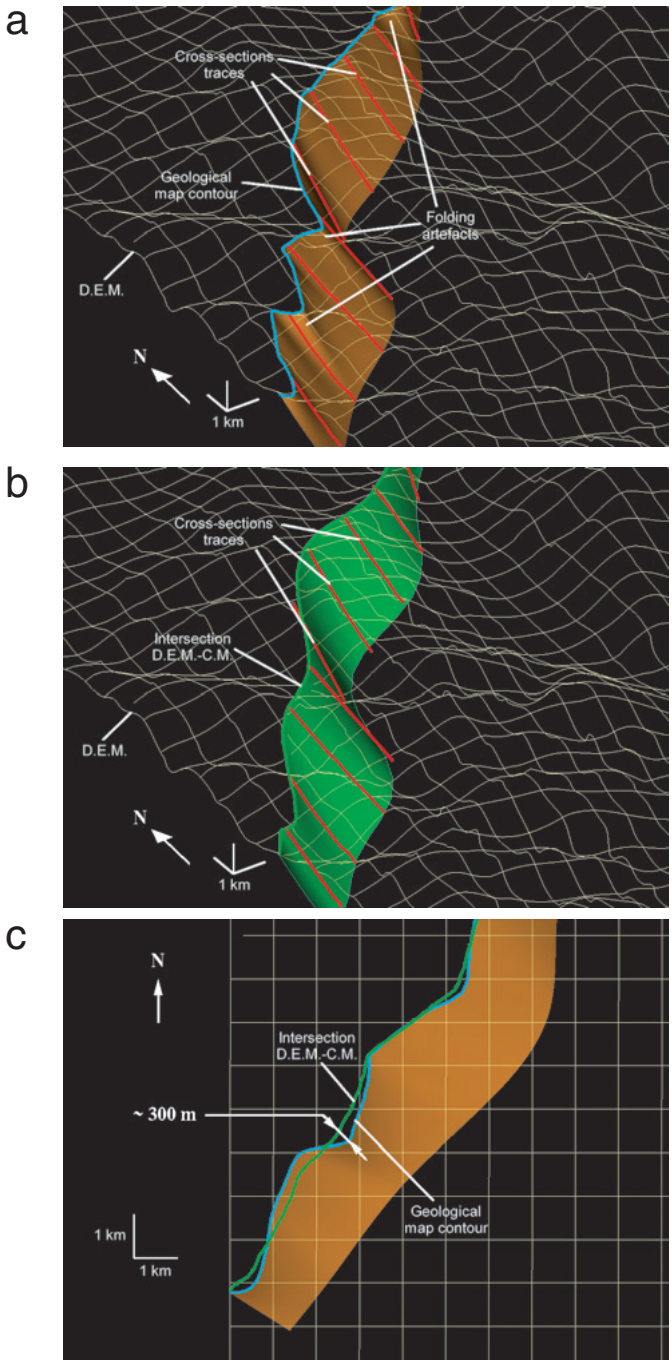

Fig. 5. Geometrical artefacts due to 3D modeling of geological interfaces: a) small-scale folding of the "accident médian"; b) 3D geometrical model of the "accident médian" based only on cross-section data; and c) projection of the two models on a horizontal grid.

ed onto the DEM grid. For the structural map, the 2D digitalized points for each cross-section were interpolated using a Bezier curve function in the plane of the cross-section. The 3D curves of the structural map are the upper limits of the interpolated interfaces crosscutting the DEM, guided by the modelled 3D curves built with respect to the geological cross-sections.

Internal coherence

With this methodology the links between serial cross-sections intersecting in the GCM area need some adjustment. In 3D modeling it is a fundamental rule that two Bezier curves defining the same interface on two secant cross-sections must intersect themselves. In fact, manual-drawing of perpendicular cross-sections in the GCM area and/or DEM structural map projections introduce imprecision that has to be corrected in the 3D model. These problems of coherence between crossing points with respect to their position on the surface structural map were solved interactively by adjusting Bezier curves to the intersection constraints.

Building of an interface: example of the "accident médian"

Two main interfaces corresponding to the "accident médian" were constructed using the methodology described above (Figs. 4a and 4b). The projection of the geological contour of this main thrust on the DEM grid corresponds to the parallel blue curves, while the traces of the cross-section appear as two red lines for each cross-section (Fig. 4a). The 3D software constructed a part of the interface surface bounded by two cross-sections and the topographic projection of the interface between these two sections. The sum of all these different surfaces leads to a Bezier surface representative of the overall structural interface in the 3D model. The lower boundary of this structural interface is constrained by the depth of the profiles on each cross-section (Fig. 4b).

Results and problems: artificial folding of interfaces

The representation of the "accident médian" resulting from this 3D model shows systematic small- scale folds beneath the valleys, which disappear with depth (Fig. 5a). This is a numerical effect, introducing periodicity, due to local misfit between geological contacts drawn on the map and the corresponding vertical cross-sections. In fact, fictive geological contacts of the "accident médian" had to be drawn below the valley's Quaternary deposits. These estimates, combined with uncertain dip values in the sections, generated small-scale corrugation of the interface at the upper surface of the 3D model.

To examine these artificial folds (artefacts), a new "accident médian" surface was constructed using only the geometry given by the cross-sections (Fig. 5b), without reference to the geological contours of the interface on the DEM. This new surface smoothes out the small-scale wavelengths (small-scale folding) but preserves the large-scale wavelength folding representative of the geological geometry of the "accident médian". Figure 5c (map view) shows horizontal projections of the cartographic traces for the constructed surfaces using cross-

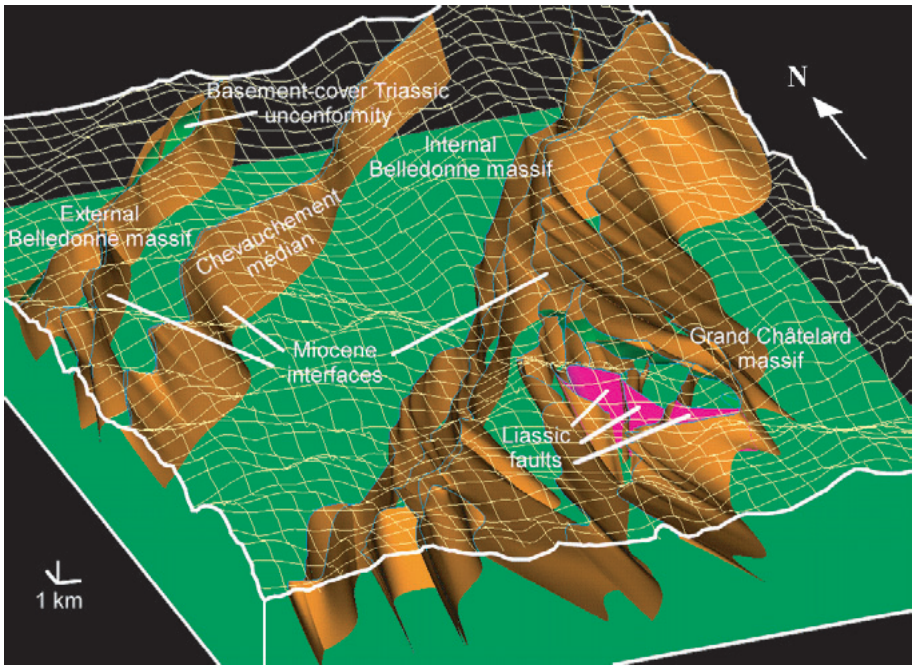

Fig. 6. 3D geometrical model of the study area. Yellow – DEM; Blue lines – geological contours on the DEM; Brown surfaces – Miocene interfaces; Purple surfaces – Liassic faults; Green surfaces – basement-cover Triassic unconformity.

sections and geological contours (Fig. 5c, blue) or only cross-sections (Fig. 5c, green). In places, the two different numerical approaches have horizontal distance misfits in the order of 300 meters.

The second solution (taking into account only the cross-sections) is not more reliable than the first one, because the new surface is based on uncertain dips in the sections. However, this comparative work shows how 3D modeling could help cartographic drawing. The ideal cartographic tool would be designed to automatically construct surfaces within defined confidence limits based on geo-referenced outcrops and structural data. The intersection of these surfaces with the DEM would give geological traces on the map view that would fit directly with the 3D model.

3D results and implications

The first advantage of changing from 2D to 3D lies in the grouping of all available data into the same space. In this way, the coherence of two data items that are related (for example by bisecting cross-sections) and which, in their respective 2D spaces, appear correct, can be definitely confirmed or invalidated by their correlation in 3D space. Based on the above methodology, Figure 6 shows a 3D view of the geometric model with the Miocene overthrusts drawn in brown, the basement-cover unconformity in green and normal faults in purple. Despite some local small-scale artificial folding, the main trends of large-scale curved interfaces can be observed from this model.

Field data should be collected with the perspective of 3D geometric modeling already in mind. The idea that the cross-sections are part of a three-dimensional issue should always be kept in view. The basic necessity is that all information is geo-referenced. In this way, all the data can be compared easily when they are merged in the common 3D space. This stage is essential for the understanding and interpretation of a complex structure. Moreover, measurements taken while collecting field data intended for three-dimensional modeling should be classified according to the modeling scale, as it will not be possible to take account of certain small-scale data during the construction of the model.

However, the methodology used for 3D modeling relies significantly on the tools currently available. This current methodology could be simplified while also limiting sources of error. For example, the transfer of data from paper to model could be avoided. This stage requires digitization of the geological parameters (either from the structural map or from cross-sections) and then their reconstruction in the model. The solution would be to use a digital structural map that could be integrated directly into the modeling software. For the cross-sections, an editing tool could be developed that would provide all the necessary information for their construction. By using the DEM and the digital geological map, this cross-section editor would offer the geologist the topographical traces of the cross-sections as well as intersections with the structural map. In addition, such an editor of 3D sections would ensure the consistency of the cross sections by automatically managing the problems of their intersection. The sections would be in a digital form that could be read by the modeler.

A second advantage of three-dimensional modeling is that it offers an easier way of testing structural hypotheses, although this can actually show some limitations in the current

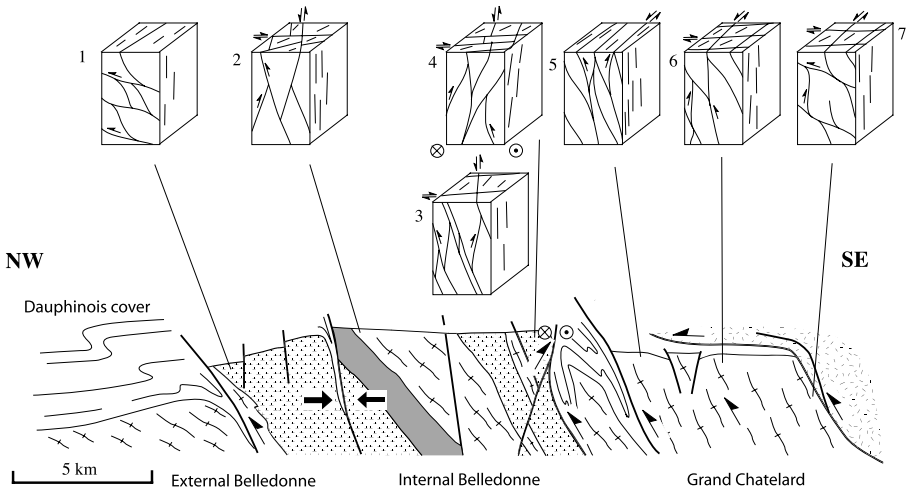

Fig. 7. NW-SE schematic cross-section of the Belledonne and Grand Châtelard massifs. Bulk kinematics of the main planar discontinuities is deduced from fault pattern analysis (measurement station numbers refer to Figs. 8 and 9; same geological patterns as on figure 2).

methodology of model construction. For example, the various interfaces of the geometric model of the Belledonne and Châtelard massifs were constructed according to the structural features of these massifs, but the model provides no intrinsic relation between the various surfaces that represent the basement-cover limit, the Miocene thrust faults and the Liassic Châtelard Fault. The modification of one of these surfaces does not necessarily affect any of the others. However, all the dependent structures have to be reconstructed, or readapted. This problem would be solved, or significantly reduced, by the inclusion of topological relations in the three-dimensional model. Adding new limitations would alter the model while maintaining the topological relations between the interfaces. The end result would then be either a single solution or a range of geometric solutions confirming (or refuting) both the initial assumption and the topological relations linking the structural interfaces.

The geometric modeling of the Belledonne and Châtelard massifs heavily relies on previously produced cross-sections. As we have seen, these cross-sections themselves represent highly interpreted data whereas, ideally, it would be best to provide the model with raw data. For the most part, this raw data would be insufficient for the geometric construction, but the model would then highlight regions of weak constraint requiring additional data, which could be obtained by local interpretation or targeted field surveys.

Geometry and kinematics of Miocene deformation

In the 3D model, some thrust planes show dip variations along the length of their strike. For example, on the south-eastern border of the BM, the dip of the basement-cover contact changes toward the NW or SE about a sub-vertical attitude. These deflections of 3D thrust surfaces, emphasised in the 3D model, need small-scale field investigations of shear zone patterns to get a better understanding of the geometry of lense-shaped domains of weakly deformed basement during Miocene deformation. Furthermore, field studies are required to ascertain whether such dip variations are the result of kinematic/mechanical effects during a single deformation phase or whether they were induced by superimposed deformations. To link the large-scale 3D approach to the internal deformation and to the geometry of the main interfaces at the boundaries of the BM and GCM, well-defined areas for studying the geometry and kinematic of the Miocene deformation were selected on a cross-section through these external Crystalline massifs. Thus, the careful observation of 3D models can redefine pertinent areas of the field study needed to explain the observed geometrical variations.

As an extension of the 3D modeling, structural and kinematic studies were carried out near the main tectonic interfaces on a NW-SE profile, at the boundaries of the BM and GCM, and around the "accident médian" (Fig. 2). During the Miocene deformation, metamorphic conditions were low-grade greenschist facies. Miocene deformation is heterogeneous in the basement rocks and leads to brittle-ductile shear zone patterns surrounding lenses of weakly deformed domains at different scales (Fig. 7). This rheological behaviour is common in basement rocks and such geometries have been widely described in numerous deformation studies of granitic rocks (Mitra 1978, 1979; Ramsay & Allison 1979; Bell 1981; Choukroune & Gapais 1983; Gapais et al. 1987; Marquer 1991; Baudin et al. 1993; Marquer et al. 1996). At the shear zone scale, numerous asymmetric structures have been used as shear sense criteria (C/S, Berthé et al. 1979; asymmetric clasts and veins, Passchier & Trouw 1996). In these local high-strain zones, the directions defined by striae, stretched minerals and preferred mineral orientations on the shear plane were assumed to be close to the displacement direction (see discussion in Gapais et al. 1987).

At the scale of the External Crystalline Massifs, a weak penetrative schistosity with N30°-N40° strike and steep dip to the SE is present in the vicinity of the main deformation zones (Fig. 8c,d, great circles). On the western boundary of the BM,

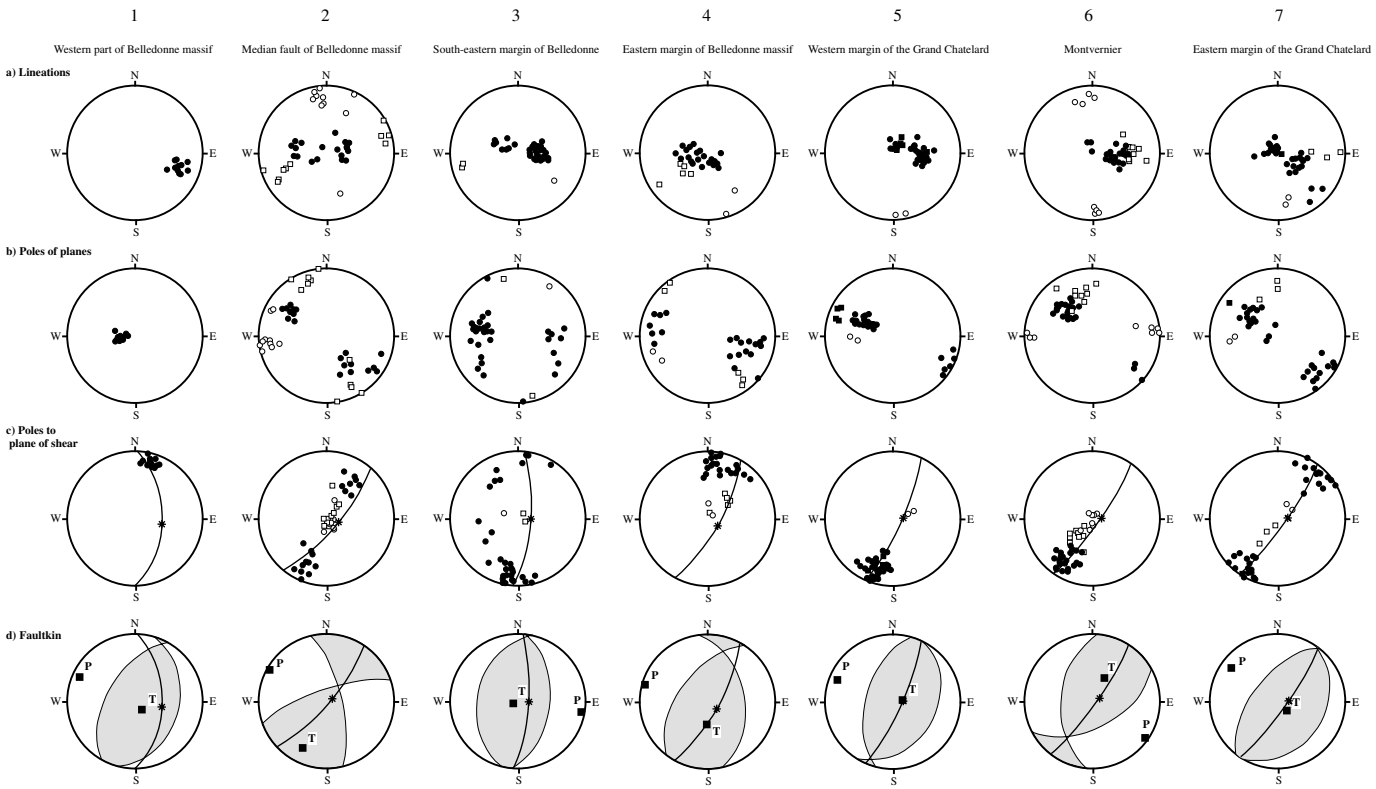

Fig. 8. Stereoplots of fault patterns from the different measurement stations: a) Lineations; b) Poles of planes; c) Poles to plane of shear. The senses of shear are as follows: open circles – sinistral zones; open squares – dextral zones; black circles – reverse zones and black squares – normal zones. The Poles to plane of shear diagrams in c) refer to the Arthaud method (see Gapais et al. 1987, Fig.3); d) Depicts the results of the Faultkin method (P and T axes calculations after Allmendinger et al. 1989). In c) and d) great circles correspond to the schistosity and asterisks to the stretching lineations for each measurement stations, respectively.

the schistosity rotates slightly, but remains steeply dipping; the schistosity direction strikes N-S and the dip of the schistosity plane is eastwards in this part of the studied area (Fig. 8). The stretching lineation, demonstrated by chlorite and quartz crystallization directions and the deformation of quartzo-feldspathic aggregates, is mainly oriented down dip on the schistosity planes (Fig. 8c,d, asterisks). The schistosity-stretching lineation couple was used as a geometrical reference for the finite strain, which enables the definition of finite strain axes X, Y and Z for each measurement station.

The studied local shear zones are considered to be coeval with the Miocene deformation because (1) they are related to the low-grade greenschist schistosity, (2) they only underwent low-grade crystallisation and (3) they show brittle-ductile deformation mechanisms. Furthermore, their spatial distribution and their kinematics are compatible with the bulk shortening and stretching defined by the occurrence of Miocene schistosity and mineral lineation, respectively, as is discussed below (Arthaud method). Only the low-grade metamorphic shear zones, which are compatible with the Miocene schistosity were considered. Previous high-grade structures in the basement rocks were avoided and not measured in the field. Neither superimposed structures nor microstructures, such as folds or crenulations, were observed in these shear zones at the scale of the investigated outcrops. This leads to the interpretation that both low-grade internal deformation and shear zones patterns at the boundaries and within the BM and GCM correspond to one progressive Miocene deformation event.

In the seven stations investigated, scattered from the western part of the BM to the south-eastern part of the GCM, conjugate sets of shear zones occur at outcrop scale and represent anastomosing shear zones along Y and X finite strain axes (Fig. 7 and 8). Dextral and sinistral shear zones strike N70°-N90° and N160°-N180°, respectively. Reverse conjugate shear zones are oriented N10°-N40° around the schistosity direction for each of the measurement stations. The compatibility of these sets of shear zones was tested using both the Arthaud method (Fig. 8c, pole to plane of shear according to Gapais et al. 1987, Fig. 3) and the Faultkin method (Fig.8d, according to the method of Angelier & Mechler 1977; Allmendinger et al. 1989). These methods, widely used in brittle tectonics, can also be used to study the geometry of ductile or brittle-ductile shear zone populations and to deduce the bulk kinematics of shear zone patterns (Gapais et al. 1987; Marquer et al. 1996). In this study, the method of kinematic fault analysis is applied to brittle-ductile shear zones and the resulting main stress axes

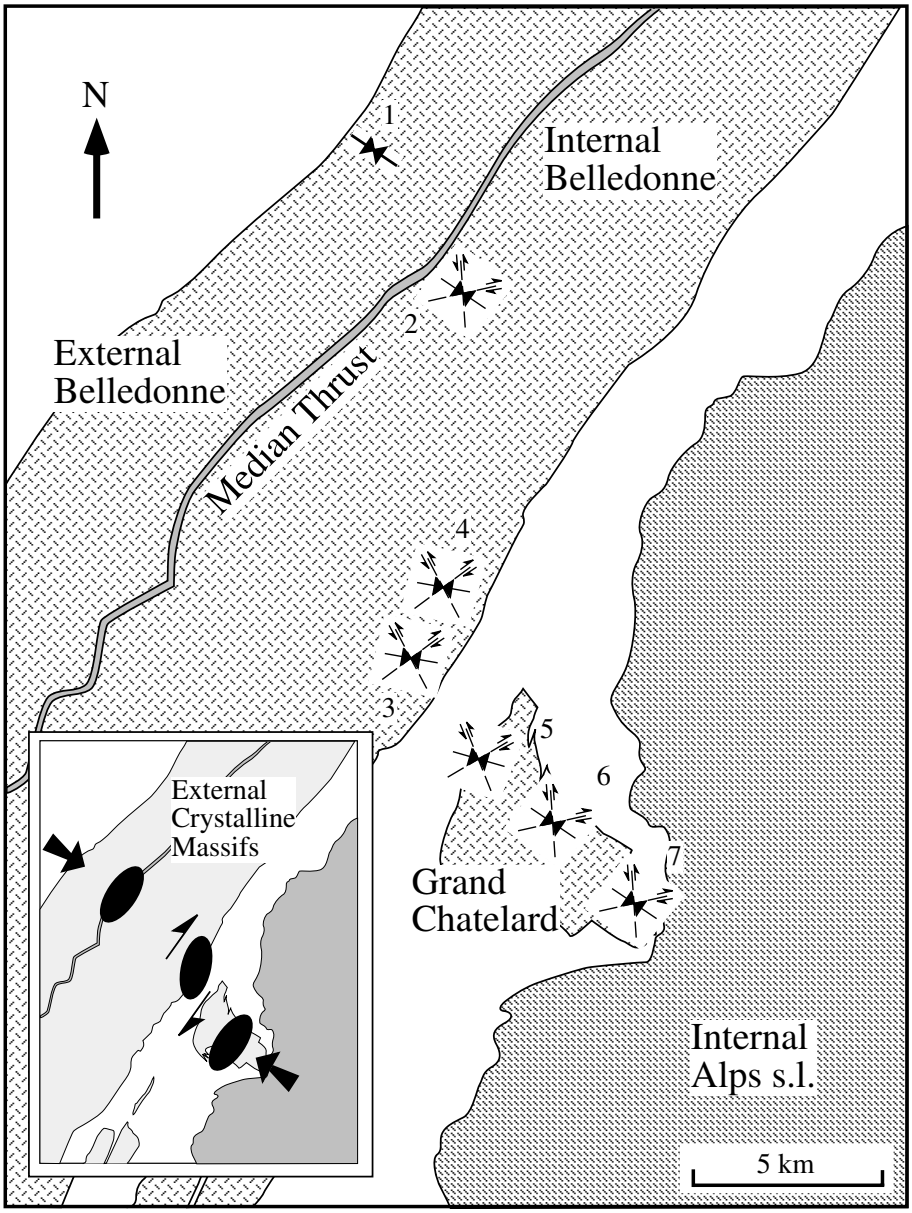

Fig. 9. Miocene brittle-ductile deformation field in Belledonne and Grand Châtelard massifs (kinematic analysis refers to the Fig. 8), showing location of measurement stations (1<7).

(P and T axes) are compared with strain axes (Z and X axes) deduced from classical strain analysis, using schistosity-stretching lineation couples measured in the lenses between the shear zones (Fig. 8). In the majority of the measurement stations, the schistosity is located in the tension field (shaded area, Fig. 8d) while the stretching lineations are close to the tension axes (see asterisks and T axes, Fig. 8c, d). The shear zone compatibility is also demonstrated by the location of the poles to the shearplanes, which in any case remain close to the great circle defined by the schistosity (Fig. 8c) (see Gapais et al. 1987).

The analysis of shear zone patterns reveals a bulk NW-SE compression (P axes), linked to vertical stretching (T axes and stretching lineations, Fig. 8) at the scale of the External Crystalline Massifs. Close to the "accident médian" zone, the high density of strike-slip shear zones observed in the field imply a horizontal position of the T tension axis while the P compression axis remains similar, as in other parts of the massifs (Station 2, Figs. 7 and 8). However, Mesozoic sediments pinched in this major overthrust imply a strong vertical component of thrusting, as attested by the other measurement stations. The results of the analysis of 3D lens-shaped domains and anastomosed faulting can be summarized on a NW-SE cross-section (Fig. 7) and at the map scale (Fig. 9). On the cross-section, conjugate shear zones emphasize NW-SE sub-horizontal shortening and the NW component of thrusting responsible for the pinching of Mesozoic sediments. Only the eastern boundary of

the BM is locally affected by retro-shear towards the south-east (Fig. 7). At the map-scale, the locally different deformation field (e.g. P axes orientations) on the eastern part of the BM (Fig. 8 and 9, stations 3 and 4) is interpreted as the result of a bulk dextral component of shearing oriented NE-SW in this area (Fig. 9).

In the southern part of the 3D model (Fig. 6), the thrust surfaces become steeper toward the GCM and some are curviplanar, tending to anastomose around the GCM. This geometrical effect creates large-scale lenses of basement similar to the small-scale boudinage phenomena shown by many metamorphic rocks or 3D described shear zone patterns. Such deflections of the 3D thrust surfaces reflect the large scale deformation pattern of the European passive margin during Miocene tectonics. Furthermore, structural analyses of these deflections could enable the prediction of basement lenses hidden at depth below the cover rocks (see NE of the Model, Fig. 6). The identification of such 3D lens-shaped domains will enable geological studies to focus on preserved zones where there are little or no effects of Miocene deformation fields. This is particularly the case for parts of the Liassic normal faults preserved on the south-east boundary of the GCM (Fig. 6, purple interfaces).

Conclusions

The use of 3D geometrical models is today an indispensable tool for solving geometrical problems in complex geological areas. Furthermore, this numerical modeling helps to discriminate potential 3D solutions and to control the geometrical coherence between different field models. On the other hand, the field data entered in these 3D models must be well chosen from geo-referenced outcrops. Cross-sections must be well constrained by high relief topography and/or sub-surface information (underground tunnels for example).

In spite of these precautions, there are some problems related to the software (Strim) and the resolution of the DEM. The current methodology requires manual-drawing of the geological data on maps and cross-sections and this leads to geological and digitalization imprecision. Whereas geologists can accommodate these imperfections from their own 3D experience, the 3D numerical model based on mathematical interpolations cannot, and therefore emphasizes the geometrical problems by producing incoherent geological results. For example, the drawing of geological contours intersecting topography in the valleys can create artificial features, such as the small scale folding of interfaces within the DEM resolution (50 m). Future solutions could include new geological software capable of drawing geological maps automatically using geo-referenced local geological observations.

The results from this test-site in the External Crystalline Massifs reveal the three dimensional relationships of the main basement-cover interfaces. This modeling technique is important for the 3D visualization and validation of field observations. For example, it provides constraints on the 3D relationships of the different interfaces where they intersect. Furthermore, it permits visualization of lens-shaped domains, together with information on variations and inversions of dips for the main thrust planes. In this way, 3D modeling can be an important tool for targeting zones for ongoing geological and structural studies.

An example of this application is given by the study of the geometry and kinematics of the Miocene tectonics in the External Crystalline Massifs. Analysis of anastomosing patterns of shear zones has led to the interpretation that this network of brittle-ductile shear zones could be compatible with a single progressive deformation. This progressive deformation corresponds to vertical stretching and NW-SE horizontal shortening during the north-west directional overthrusting of the BM and GCM. Locally, the south-eastern margin of the BM was affected by a NE-SW dextral retro-shear component, leading to local inversion of the dip of this interface as previously visualised on the 3D model.

In the future, this kind of 3D geometrical model will enable volumetric visualization in well-defined areas with sufficient topographic relief. Numerous applications in different branches of geosciences will use such a three dimensional tool to quantify potential reservoirs of rocks, fluids, and mineralization as well as constructing 3D geophysical inversion models for well-defined 3D domains. This approach could also be linked with 3D restoration software to acquire information on the geometry of undeformed objects such as, in our case, the Liassic European margin.

Acknowledgements:

This work was funded by the Géofrance3D program, Publication n° 106. We thank N. Mancktelow, M. Burkhard and S. Schmid for helpful and constructive reviews.

REFERENCES

Allmendinger, R.W., Marrett & R.A., Cladouhos, T., 1989: Fault kinematics: a program for analysing fault slip data for the Macintosh computer. Cornell University, Ithaca, 34p.

Angelier, J. & Mechler, P., 1977: Sur la méthode graphique de recherche des contraintes principales également utilisable en tectonique et en séismologie: la méthode des dièdres droits. Bull. Soc. géol. France XIX, 6, 1309–1318.

Barbier, R., 1944: Sur l'existence d'un dôme émergé au Lias inférieur dans le Massif du Grand-Chatelard (Rocheray) près de St-Jean de-Maurienne (Savoie). C. R. Somm. Soc. géol. France 4, 38–39.

Barbier, R., 1956: L'importance de la tectonique anté-nummulitique dans la Zone Ultra-Dauphinoise au Nord du Pelvoux: la chaîne arvinche. Bull. Soc. géol. France 6, 355–370.

Barféty, J.C., 1985: Le Jurassique dauphinois entre Durance et Rhône, étude stratigraphique et géodynamique (zone externe des Alpes occidentales), Documents BRGM 131, 665 p.

Barféty, J.C. & Gidon, M., 1984: Un exemple de sédimentation sur un abrupt de faille fossile: le Lias du versant est du massif du Taillefer (Zone Dauphinoise, Alpes occidentales). Rev. Géol. Dyn. et Géo. Phys. Paris 25, 267–276.

Barféty, J.C. & Gidon M., 1990: La tectonique alpine du massif cristallin du Taillefer (Alpes occidentales françaises): découverte de chevauchement vers le Nord, Géologie alpine 66, 1–9.

Barféty, J.C., Barbier, R., Bordet, P., Fabre, J., Petiteville, J., Rivoirard, R., Vatin-Pérignon, N., Mouterde & R., Méloux, J., 1977: Carte géol. France (1/50000), Saint-Jean-de-Maurienne (774). Orléans BRGM. Notice explicative par Barféty J.C. et al. (1977), 43 p.

Barféty J.C., Barbier, R., Antoine, P., Blaise, J., Bordet, P., Mouterde, R., Fourneaux, J.C., Montjuvent, G., Amat-Chantoux, R., Pappini, G., Liard, P., Méloux, J.& Cabrol, B., 1983: Carte géol. France (1/50000), feuille La Rochette (750). Orléans BRGM. Notice explicative par Barféty J.C. et al. (1984), 45 p.

Baudin, Th., Marquer, D. & Persoz, F., 1993: Basement-cover relationships in the Tambo nappe (Central alps, Switzerland): geometry, structures and kinematics. J. Struct. Geol. 15, 3/5, 543–553.

Bell, T.H., 1981: Foliation development: the contribution, geometry and significance of progressive bulk, inhomogeneous shortening. Tectonophysics 75, 273–296.

Berthé, D., Choukroune, P. & Jégouzo, P., 1979: Orthogneiss, mylonite and non coaxial deformation of granites: example of the South Armorican shear zone. J. Struct. Geol. 1, 31–42.

Bucher S., Ulardic, C., Bousquet R., Ceriani, S., Fügenschuh B. & Schmid, S. M., 2004: Tectonic evolution of the Briançonnais units along the ECORS-CROP transect through the Italian-French Western Alps. Eclogae geol. Helv. 97, 321–345.

Ceriani, St., Fügenschuh, B. & Schmid, S.M., 2001: Multi-stage thrusting at the "Penninic Front" in the Western Alps between Mont Blanc and Pelvoux massifs. Int. J. Earth Sciences 90, 685–702.

Ceriani, S. & Schmid, S.M., 2004: From N-S collision to WNW-directed post-collisional thrusting and folding: Structural study of the Frontal Penninic Units in Savoie (Western Alps, France). Eclogae geol. Helv. 97, 347–369.

Choukroune, P. & Gapais, D., 1983: Strain pattern in the Aar granite (central Alps); orthogneiss developed by bulk inhomogeneous flattening. J. Struct. Geol. 5, 3/4, 411–418.

Courrioux, G., Nullans, S., Guillen, A., Boissonat, J.-D., Repusseau, Ph., Renaud, X. & Thibaut, M, 2001: 3D volumetric modelling of Cadomian terranes (Northern Britanny, France): an automatic method using Voronoi diagrams. Tectonophysics 331, 1–2, 181–196.

Crouzet, C., 1997: Le thermopaléomagnétisme: méthodologie et applications (tectonique, thermique et géochronologique) à la zone Dauphinoise (Alpes Occidentales, France). Géologie Alpine, Mémoire HS n°27, 197p.

Cuenin, R., 1972: Cartographie générale. Tome 1: notions générales et principes d'élaboration. Collection scientifique de l'IGN, Eyrolles Ed., Paris.

Debelmas, J. & Lemoine, M., 1970: The western Alps: palaeogeography and structure. Earth Sci. Rev. 6, 221–256.

De Kemp, A., 1999: Visualization of complex geological structures using 3-D Bézier construction tools. Computers and Geosciences 25/5, 581–597.

Forrest, A.R., 1990: Interactive interpolation and approximation by Bézier polynomials. Computer aided design 22/9, 527–537.

Fügenschuh, B., Loprieno, A., Ceriani, St. & Schmid, S.M., 1999: Structural analysis of the Subbriançonnais and Valais units in the area of Moûtiers (Savoy, Western Alps): paleogeographic and tectonic consequences. Int. J. Earth Sciences 88, 201–218.

Fügenschuh, B. & Schmid, S.M., 2003: Late stages of deformation and exhumation of an orogen constrained by fission track data: A case study in the Western Alps. Geological Society of America Bulletin 115 1425–1440.

Gapais, D., Balé, P., Choukroune, P., Cobbold, P., Mahdjoub, Y. & Marquer D., 1987: Bulk kinematics from shear zone patterns; some field examples. J. Struct. Geol. 9, 5/6, 635–646.

Hamilton, D.E. & Jones, T.A., 1992: Computer Modeling of Geologic Surfaces and Volumes. AAPG Computer Applications in Geology 1, 297 pp.

Houlding, S. W., 1995: 3D Geoscience Modeling, Computer Techniques for Geological Characterization. Springer-Verlag, 310 p.

Jessell, M.W. & Valenta, R.K., 1996: Structural geophysics: Integrated structural and geophysical modeling. (Ed. by De Paor, D.G.), Structural Geology and Personal Computers. Pergamon Press, Oxford, 303–323.

Leloup, P.H., Arnaud, N., Sobel, E.R. & Lacassin, R. 2005: Alpine thermal and structural evolution of the highest external crystalline massif: The Mont Blanc. Tectonics 24, TC4002, doi: 10.1029/2004TC001676.

Marquer, D., 1991: Structures et cinématique des déformations alpines dans le granite de Truzzo (Nappe de Tambo: Alpes centrales suisses). Eclogae geol. Helv. 84/1, 107–123.

Marquer, D., Challandes, N. & Baudin, Th., 1996: Shear zone patterns and strain partitioning at the scale of a Pennine nappe: the Suretta nappe (eastern Swiss Alps). J. Struct. Geol. 18/6, 753–764.

Menard, G. & Rochette, P., 1992: Utilisation de réaimantations postmétamorphiques pour une étude de l'évolution tectonique et thermique tardive dans les Alpes occidentales (France). Bull. Soc. géol. France 163/4, 381–392.

Menard, G. & Thouvenot, F., 1987: Coupes équilibrées crustales: méthodologie et application aux Alpes occidentales. Geodinamica Acta 1/1, 35–45.

Mitra, G., 1978: Ductile deformation zones and mylonites; the mechanical processes involved in the deformation of crystalline basement rocks. Amer. J. Science 278, 1057–1084.

Mitra, G., 1979. Ductile deformation zones in Blue Ridge basement rocks and estimation of finite strains. Geol. Soc. Amer. Bull., Part I, Vol. 90, 935–951.

Nziengui, J.J., 1993: Excès d'argon radiogénique dans le quartz des fissures tectoniques: implications pour la datation des séries méthamorphiques. L'exemple de la coupe de la Romanche, Alpes Occidentales françaises. Thèse 3ème cycle, Université Joseph Fourier, Grenoble 1, France, 209 p.

Passchier, C.W. & Trouw, R.A.J., 1996: Micro-tectonics. Springer-Verlag, Berlin, 289p.

Ramsay J.G. & Allison, N.I., 1979: Structural analysis of shear zones in an Alpinised Hercynian granite (Maggia Lappen, Pennine zone, Central Alps). Schweiz. Mineral. Petrogr. Mitt. 59, 251–279.

Schmid, S.M., Fügenschuh, B., Kissling, E. & Schuster, R. 2004: Tectonic map and overall architecture of the Alpine orogen. Eclogae geol. Helv. 97, 93–117.

Seward, D. & Mancktelow, N.S., 1994: Neogene kinematics of the Central and Western Alps: evidence from fission-track dating. Geology 22, 803–806.

Tricart, P., 2004: From extension to transpression during final exhumation of the Pelvoux and Argentera massifs, Western Alps. Eclogae geol. Helv. 97, 429–439.

Manuscript received March 9, 2006
Revision accepted April 21, 2006
Published Online First August 14, 2006